Toluene Model for Molecular Dynamics Simulations in the Ranges 298 < *T* (K) < 350 and 0.1 < *P* (MPa) < 10

Marco Fioroni and Dieter Vogt*

Eindhoven University of Technology, Schuit Institute of Catalysis, Lab. of Hom. Catalysis, Helix Building, SKA, P.O. Box 513, 5600 MB Eindhoven, The Netherlands

Received: November 26, 2003; In Final Form: May 18, 2004

An all-atom model for toluene is presented in the framework of classical molecular dynamics (MD). The model has been parametrized under the GROMOS96 force field to reproduce the physicochemical properties of the neat liquid. Four new atom types have been introduced, distinguishing between carbons and hydrogens of the aromatic and of the CH_3 aliphatic groups. The thermodynamic and kinetic properties in the liquid phase have been calculated within a temperature and a pressure range of 298 < *T* (K) < 350 and 0.1 < *P* (MPa) < 10, respectively. The average relative deviations from the experimental data in the range of temperatures and pressures considered are 0.5%, 7% and 25% for the density, vaporization enthalpy and viscosity, respectively. The free energy of hydration has been estimated as −5.8 kJ mol^{-1}, in good agreement with the experimental value of −3.6 kJ mol^{-1}. Structural investigations have been conducted to understand the structure of the liquid and compared to experimental data. Parallel stacking of the aromatic planes with antiparallel disposition of the CH_3 groups has been found. The presented toluene model is suitable for MD simulations in a range of pressures and temperatures interesting for industrial processes and organic chemistry (i.e., polymer and dendrimer dynamics).

1. Introduction

Liquid toluene is one of the most commonly used nonpolar aromatic solvents in synthetic organic chemistry and in industrial processes. The lesser carcinogenic action of toluene has increased its use replacing benzene, as it also shows very similar solvation characteristics. The macroscopic properties of liquid toluene (i.e., density, viscosity, isothermal compressibility, thermal expansion coefficient, heat capacity, and thermal conductivity)[1] have been extensively studied in a wide range of temperatures and pressures, because of its importance as a possible primary reference standard for the conductivity of liquids[2] or viscosity measurements.[3] Another source of interest is due to the analysis of the glass-forming materials, toluene being one of the simplest ones.[4] However, despite the large use, little is known on the reasons why toluene molecules can facilitate chemical reactions or on the microscopic properties as structure and solvation dynamics.[5,6] In the last few years greater efforts have been devoted to unravel these microscopic properties. Light scattering,[1] THz spectroscopy[7] and ^{13}C NMR relaxation studies[6] have been widely applied to understand the intra and intermolecular dynamics in neat liquid toluene. Parallel to the enhanced experimental research, a growing theoretical interest in toluene is appeared.[8−11] However, while great attention has been paid to the parametrization of benzene molecules under different force fields,[12,13] able to reproduce properly the thermodynamic, kinetic, and even spectroscopical properties[13] of the pure liquid, toluene has not received the same consideration. The main theoretical interest for toluene comes out being a better model of the $\pi-\pi$ interactions in proteins, represented by the phenylalanine.[8−10] For these reasons, the main studies on toluene are concentrated on the dimer in the gas phase or in a host liquid interactions, to understand which of the possible forms (T-shaped or stacked) are the most stable.[8−10] The liquid state has received less attention,[11,14,15] although many simulations on polymers solvated in toluene have been reported.[14,16] Regarding the force fields, united model atoms for the linear and branched alkenes and alkylbenzenes have been proposed[17] in parallel with the OPLS united-atom force field[18] and the all-atom version.[12,19] The need to enhance, modify, or create new force fields, comes out from the wider range of physical conditions (temperature and pressure) in which the solute/solvent systems are required to work properly,[20,21] especially considering industrial processes, quite often distant from normal conditions (298 K and 1 bar). For example, the OPLS force field[18,19] works excellently reproducing the liquid properties of a great variety of chemical compounds, but some limitations have been found when it is applied to long chain alcohols or when simulations at elevated temperature[22] and pressure of saturated, unsaturated and aromatic hydrocarbons are considered. From previous experiences of one of the authors on the parametrization of other solvents,[23−25] the inclusion of kinetic properties in the parametrization scheme has been found to be extremely important. In fact, while thermodynamic properties of the model liquids (i.e., density, pressure, enthalpy of vaporization, compressibility) can be satisfied from a different set of values for the long-range interactions, the kinetic properties (diffusion, rotational dynamics, dielectric constant) are more sensible and restrictive. Regarding the GROMOS96 FF, the functional form does not include a polarization term. The nonexisting term of polarizability in the FF should not, however, deeply affect the properties of the toluene model when used as a solvent, apart from when interactions with ions and in-vacuum simulations of ion−toluene clusters are considered. Previous studies on benzene models have shown the aforementioned behavior.[26,27] Kinetic quantities such as the viscosity and/

* Corresponding author. Telephone: +31-40.2472730. Fax: +31-40.2455054. E-mail: d.vogt@tue.nl.

10.1021/jp037605c CCC: $27.50
Published on Web 07/03/2004

TABLE 1: Optimized B3LYP/6-31+G(d,p) Geometry Values for Toluene in Vacuum, Where the Subscripts ar and al Refer to the Aliphatic and Aromatic Atoms

atoms	
$r(C_{ar}-C_{ar})$[a]	0.1395
$r(C_{ar}-C_{al})$	0.1509
$r(C_{ar}-H_{ar})$	0.1080
$r(C_{al}-H_{al})$	0.1091
$\theta(C_{ar}-C_{ar}-C_{ar})$[b]	120.57
$\theta(C_{ar}-C_{ar}-C_{al})$	121.23
$\theta(H_{ar}-C_{al}-C_{ar})$	120.34
$\theta(H_{al}-C_{al}-C_{ar})$	111.13
$\theta(H_{al}-C_{al}-H_{al})$	107.82
$\phi(C_{ar}-C_{ar}-C_{ar}-C_{ar})$	0.0
$\phi(C_{ar}-C_{ar}-C_{ar}-H_{al})$	180.0
$\phi(H_{ar}-C_{ar}-C_{ar}-H_{ar})$	0.0
$\phi(C_{al}-C_{ar}-C_{ar}-H_{ar})$	180.0

[a] Distances in nanometers. [b] Angles in degrees. [c] Dihedrals in degrees.

or diffusion can be considered of major importance for the behavior of polymer studies/simulations, quantities where our toluene model has been parametrized with attention. For all of these reasons, the proposed new toluene model has been developed following two purposes. The first one concerns the implementation of a model able to reproduce the thermodynamic and kinetic experimental data in a range of pressure and temperature widely used in organic and industrial fields. This target will allow to expand the use of the toluene model especially in the field of polymer simulation[14,16] or organometallic compounds. The second purpose is a first step to include new atom types in the GROMOS96 force field, to treat the explicit hydrogens and carbons of the aromatic and aliphatic groups out of the united model.

2. Methods

2.1. Toluene Force Field. The force field parameters for toluene were developed considering the reproducibility of the liquid properties. All the simulations have been carried out using the GROMACS 3.1[28] simulation package based on the GROMOS96 force field.[29] The toluene geometrical parameters were obtained from an optimized structure at the B3LYP level[30,31] with a 6-31+G(d,p) basis set[32] (see Table 1). The geometric parameters taken from the GROMOS96 and the calculated ones are nearly coincident. Bonds have been constrained to fixed distances. In fact, some of the considered bulk liquid properties of toluene (i.e., enthalpy of vaporization, density, and viscosity), kept as reference parameters during the parametrization protocol, are little affected by the exclusion of the C−C and C−H stretching modes. These stretching modes show higher frequencies (>400 cm^{-1}) compared to the higher intermolecular vibrations (<200 cm^{-1}), which affect the dynamics of the condensed phase. When vibrations are important like in the heat capacity estimation, bond vibrational corrections have been introduced. The partial atomic charges were calculated within the Gaussian98 package[33] using the CHELPG procedure,[34] which has been shown to give a good evaluation of the partial charge values used in MD force fields.[35] In Table 2, the charges obtained from the B3LYP level calculations are reported. The calculated charges as obtained from the density functional calculations have been applied to the MD model to reproduce the dipole/quadrupole moments of toluene. These moments can be well reproduced from the simple monopoles in an acceptable accuracy.[10] The importance of the dipole/quadrupole interactions come out, together with the dispersive interactions, because of their ability to mimic the $\pi-\pi$ interactions in the classical force

TABLE 2: Force Field Parameters for the Toluene Model[a]

atom type	$C^6_{i,i}$/(kJ mol^{-1} nm^6) × 10^3	$C^{12}_{i,i}$/(kJ mol^{-1} nm^{12}) × 10^6	q/e
C_{ar}	2.40	4.38	0.250
$C_{ar,o}$	2.40	4.38	−0.223, −0.223
$C_{ar,m}$	2.40	4.38	−0.045, −0.034
$C_{ar,p}$	2.40	4.38	−0.128
C_{al}	1.65	3.38	−0.278
$H_{ar,o}$	0.1003654	0.0196	0.113, 0.075
$H_{ar,m}$	0.1003654	0.0196	0.075, 0.085
$H_{ar,p}$	0.1003654	0.0196	0.108
H_{al}	0.1174270	0.0258	0.079, 0.073, 0.073
dipole			0.36 (0.31)

bond	distance (nm)	bond	distance (nm)
$r(C_{ar}-C_{ar})$	0.1390	$r(C_{ar}-H_{ar})$	0.1080
$r(C_{ar}-C_{al})$	0.1500	$r(C_{al}-H_{al})$	0.1093

bond angle	θ_0 (deg)	K_θ (kJ mol^{-1})
$\theta(C_{ar}-C_{ar}-C_{ar})$	120.00	414.20
$\theta(C_{ar}-C_{ar}-C_{al})$	120.00	460.24
$\theta(C_{ar}-H_{ar}-C_{ar})$	120.00	376.56
$\theta(H_{al}-C_{al}-C_{ar})$	120.00	376.56
$\theta(H_{al}-C_{al}-H_{al})$	120.00	334.72

improper dihedrals	ϕ_0 (deg)	K_ϕ (kJ mol^{-1} deg^{-2})
$\phi(C_{ar}-C_{ar}-C_{ar}-C_{ar})$	0.00	167.42309
$\phi(C_{ar}-C_{ar}-C_{ar}-C_{al})$	180.00	167.42309
$\phi(C_{ar}-C_{ar}-C_{ar}-H_{ar})$	180.00	167.42309
$\phi(H_{ar}-C_{ar}-C_{ar}-H_{ar})$	0.00	167.42309

[a] Atom nomenclature as in the previous table. The o, m, and p subscripts refer to ortho, meta, and para positions to the opposite sites. The charge units and the dipole units are electrons and Debye, respectively. Experimental data are given in parentheses.

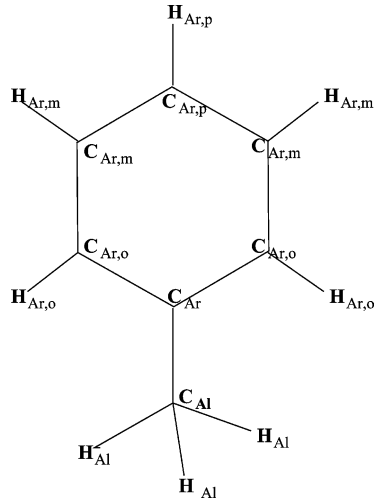

Figure 1. Atom names used in the toluene model.

fields.[8,10] In Figure 1, the atom names used in the model are reported. The Lennard-Jones (LJ) interaction parameters between two atoms were calculated as the geometric mean of the LJ parameters of the corresponding atom types, i.e., $C^{\alpha}_{1,2} = \sqrt{C^{\alpha}_{1,1} C^{\alpha}_{2,2}}$ with $\alpha = 12$ or 6, and index 1 or 2 referring to the different atom species. The parameters for the bare carbon (atom type C) and the corresponding bonded hydrogens (atom type HC) were used. The nonbonded interactions were the standard present in the force field. The resulting toluene liquid density, $\rho = 954.7$ kg/m^3, the enthalpy of vaporization, $\Delta H_{vap} = 43.05$ kJ $mol^{-1}$and the viscosity $\eta = 655$ μPa s at 298 K and 1 bar pressure, were found to be all too distant compared to the experimental data; 862.9 kg/m^3, 38.06 kJ mol^{-1} and 559.5 μPa

s for the density, enthalpy of vaporization, and viscosity, respectively. To obtain a toluene model able to reproduce the selected macroscopic variables, the LJ values have been systematically modified, introducing a difference between the carbons and hydrogens of the aromatic and the methyl group. It should be noted that the GROMOS96 force field shows no differences between the aromatic or aliphatic bare carbons and relative bare hydrogens, a difference which is present in the united atom models. Starting with the LJ values of the C and H atom types, all the following modified values of the C_6 and C_{12} LJ parameters for aromatic and aliphatic carbons and hydrogens, have been deduced from the relative ratio of the C_6 and C_{12} considering the CH_1 united atom model of the GROMOS96 force field. For C_6, Ar/Al = 1.46, and for C_{12}, Ar/Al = 1.33. The changing of the LJ values has been applied considering ratios near the aforementioned values able to reproduce the selected thermodynamic and kinetic properties. Other force fields such as AMBER[36] show nearly the same proportions. Although the selected force field setting is quite empirical, this procedure should avoid better the inclusion of atom types which are not consistent with other atom types of the force field. Besides, using a more "physical" derivation of the LJ parameters based on the atomic hybrid components method,[37] ratios with nearly same values have been obtained. The calculation of the free energy of hydration (ΔG_{hyd}), can be a test for the evaluation of the cross interactions between the new atom types and water (SPC model[38]). In fact, an obtained good value of the ΔG_{hyd} is a clue to the validity of the introduced parameters governing the new molecule.[39] The inclusion of viscosity as a third parametrization variable is due to the sensibility of this property toward the selected LJ parameters. While the reproducibility of density and enthalpy can be satisfied from different parameter values, the inclusion of the kinetic properties as the viscosity gives less freedom to the possible range of values used to satisfy the experimental data.[25] The validity of the model has been quantified considering the RMSD (root mean square deviation) or σ

$$\sigma = \sqrt{\frac{1}{n}\sum_{n}(x_{n,\mathrm{exp}} - x_{n,\mathrm{calc}})^2} \tag{1}$$

the relative RMSD or $\sigma(\%)$

$$\sigma(\%) = 100^* \sqrt{\frac{1}{n}\sum_{n}\left(\frac{x_{n,\mathrm{exp}} - x_{n,\mathrm{calc}}}{x_{n,\mathrm{exp}}}\right)^2} \tag{2}$$

and the mean deviation or bias

$$\mathrm{bias} = \frac{1}{n}\sum_{n}(x_{n,\mathrm{exp}} - x_{n,\mathrm{calc}}) \tag{3}$$

between experimental (exp) and calculated (calc) data on n considered points of the variable x, where $x = \Delta H_{vap}$, ρ, or η.

2.2. MD Simulations. The neat liquid was simulated at different temperatures and pressures under NpT conditions using a periodic cubic simulation box containing 216 or 432 molecules. The parameters used for the simulations are reported in Tables 3 and 4. In all simulations the temperature was maintained close to the reference value by a Nosé−Hoover thermostat[40] with a time constant of $\tau_T = 1$ ps. The pressure was maintained by a Parrinello−Rahmann barostat with a time constant of $\tau_P = 7$ ps[41] and the compressibility of toluene fixed to (9.7×10^{-5} bar^{-1}).[42] Lattice parameters of the cubic box were controlled for all the simulations and a uniform dilatation and contraction was checked and obtained. Besides, different starting configuration of the boxes have been taken to test the ergodicity of the system. The final results were in agreement within the fluctuations of the considered parameters. The LINCS algorithm[43] was used to constrain all bond lengths in toluene. For the water molecules, the SETTLE algorithm was used.[44] In simulations performed with a reaction-field correction, the value of ϵ_{RF} was set to the experimental dielectric permittivity of the simulated system ($\epsilon = 2.38$).[42] In simulations performed using a twin range cutoff for the calculation of the nonbonded interactions, all interactions within a short range cutoff of 0.8 nm were updated every step whereas all interactions (Coulomb

TABLE 3: Summary of the Simulations of the Pure Toluene[a]

T (K)	simul time (ns)	N_{tol}	conditions	ρ (kg m^{-3})	p (bar)	ΔH_{vap} (kJ mol^{-1})
298_{RF}	3	216	*NpT*	864.1 ± 9.1	1.9	36.5 ± 0.5
$298_{cut-off}$	3	216	*NpT*	863.9 ± 8.2	1.1	36.4 ± 0.25
298_{RF}	3	432	*NpT*	863.5 ± 6.9	1.8	36.5 ± 0.4
$298_{cut-off}$	3	432	*NpT*	863.4 ± 7.1	1.7	36.4 ± 0.24
298_{RF}	3	216	*NpT*	868.2 ± 9.6	50.7	36.7 ± 0.5
298_{RF}	3	216	*NpT*	872.0 ± 9.1	101.0	36.9 ± 0.5
322_{RF}	3	216	*NpT*	837.5 ± 9.9	1.2	34.6 ± 0.7
322_{RF}	3	216	*NpT*	842.7 ± 10.9	51.1	34.9 ± 0.7
322_{RF}	3	216	*NpT*	847.0 ± 11.2	101.2	35.1 ± 0.7
350_{RF}	3	216	*NpT*	805.2 ± 10.5	1.2	31.5 ± 0.9
350_{RF}	3	216	*NpT*	810.8 ± 11.4	50.5	31.8 ± 0.9
350_{RF}	3	216	*NpT*	816.9 ± 11.9	100.4	32.1 ± 0.9

exp[2]	p (bar)	ρ (kg m^{-3})
298	1.0	862.9
298	50.0	866.7
298	100.0	870.7
322	1.0	840.2
322	50.0	844.6
322	100.0	848.9
350	1.0	813.3
350	50.0	818.4
350	100.0	823.3

exp[45]	ΔH_{vap} (kJ mol^{-1})
298	38.06
322	36.71
350	35.15

[a] The subscript RF denotes the simulation performed using the reaction field. The standard deviations of the density and vaporization enthalpy are reported in the table. The standard deviations for the pressures and temperatures are 250 and 350 bar for the boxes of 216 and 432 molecules and 7 K for both systems.

TABLE 4: Summary of the Calculated Viscosities of the Pure Toluene at Different Temperatures and Pressures[a]

T (K)	p (bar)	β_{calc} (μPa s)	β_{exp}[d] (μPa s)
298_{RF}	1.0	436.7 ± 11.1	559.5
$298_{cut-off}$	1.0	400.2 ± 11.8	559.5
298_{RF}	50.0	444.2 ± 11.3	581.8
298_{RF}	100.0	476.2 ± 11.8	605.9
322_{RF}	1.0	300.7 ± 11.4	427.3
322_{RF}	50.0	313.1 ± 11.6	444.9
322_{RF}	100.0	324.3 ± 11.5	462.8
350_{RF}	1.0	250.1 ± 11.9	328.1
350_{RF}	50.0	261.0 ± 11.6	342.2
350_{RF}	100.0	266.3 ± 11.5	356.1

[a] The standard errors are reported in the table. In the case of experimental quantities, the uncertainty is 0.5%.[2]

and Lennard-Jones) within a long range cutoff of 1.4 nm were updated only every five steps together with the pair list. The cutoff values are in accord with those standardly used in the GROMOS96 force field.[29] A dielectric permittivity of $\epsilon_r = 1$ and a time step of 2 fs were used. For all the simulations, the systems were first minimized at the beginning for 100 steps using the steepest descent algorithm to eliminate unfavorable contacts and assigning the initial velocities from a Maxwellian distribution corresponding to the selected temperature. Previous relaxation and equilibration of the systems have been reached performing simulations for 300 ps. After equilibration, simulation runs of 2 ns were used for the viscosity estimation and 3 ns was used for all the other analysis.

3. Physicochemical Properties

3.1. Thermodynamic Properties. Density. The densities of toluene calculated at different temperatures and pressures are reported in Table 3 together with the experimental one.[2] The overall agreement with the experimental data is good. In the range of 1−100 bar of pressure, at the temperature of 298 K the model shows a σ of 1.34 kg/m^3, a σ(%) of 0.15%, and a mean deviation of −1.33 kg/m^3 and at 322 K a σ of 2.20 kg/m^3, a σ(%) = 0.26%, and a mean deviation of 2.17 kg/m^3. At 350 K, σ = 7.40 kg/m^3 and σ(%) = 0.90% with a mean deviation of 7.36 kg/m^3. However, these last reported errors are still acceptable considering the more "extreme conditions".

Enthalpy of Vaporization. The enthalpy of vaporizations, ΔH_{vap}, as reported in Table 3 were estimated as

$$\Delta H_{vap} = [U_{inter}(g) - U_{inter}(l)] + [U_{intra}(g) - U_{intra}(l)] + p\Delta V \quad (4)$$

where $U_{inter}(g)$ is the total potential energy for the interatomic nonbonded interactions and U_{intra} is the intramolecular energy (angles, torsions, intramolecular nonbonded interactions). $U_{inter}(g)$ was assumed to be zero while $U_{intra}(g)$ was calculated by averaging over a number of independent simulations of isolated molecules. The experimental values have been deduced from the relation[45] (for 1 bar external pressure):

$$\Delta H^0_{vap} = A \exp(-\beta T_r)(1 - T_r)^{\beta} \quad (5)$$

where $T_r = T/T_c$ with T_c = 591.7 K (critical temperature), β = 0.2774, and A = 53.09 kJ mol^{-1}.

The vaporization enthalpy is always lower compared to the experimental data with a σ of 2.6 kJ mol^{-1}, a σ(%) of 7.34%, and a mean deviation of 2.44 kJ mol^{-1} calculated on all the temperature intervals. As shown in Table 3, the densities and enthalpy of vaporization of toluene model are not influenced by the box dimensions or by the electrostatic treatment.

Heat Capacity. The heat capacity at constant pressure C_P was calculated using the approach described in Chelli et al.[46] Basically, the thermodynamic properties in the condensed phase can be split into a sum of two quantities: the configurational and the vibrational contributions.[47,48] The configurational contribution is linked to the *inherent structure* concept,[47,48] i.e., the structure represented by a local minimum of the many-body system reached by a steepest descent minimization, with the vibrational part sampled around the inherent structure itself. In fact, the quantum behavior of the hydrogen atoms, i.e., stretching and bending modes, with characteristic temperatures of $T \approx$ 1000 K, leave practically unchanged the vibrational states in the range of temperatures considered (298−350 K). The MD simulations based on classical potentials couple to each degree of freedom, a kinetic energy of $k_BT/2$, with the population of the states increasing linearly with T and the statistics represented by the Maxwell theory, while the Bose−Einstein theory should be the right one when quantum systems are considered. On the basis of the previous considerations, the heat capacity calculated through a classical estimation can bring to considerable errors. The inherent structure concept can be a useful solution to this problem. The C_P can be written/split as

$$C_P = C_P^{conf} + C_P^{vibr} \quad (6)$$

where C_P^{conf} is equal to

$$C_P^{conf} = \left(\frac{\delta H_{conf}}{\delta T}\right)_P = \left(\frac{\delta E_{conf}}{\delta T}\right)_P + P\left(\frac{\delta V}{\delta T}\right)_P \quad (7)$$

and C_P^{vibr} to

$$C_P^{vibr} = n_f R \int_0^{\infty} g(T,\nu) \frac{(h\nu/kT)^2 e^{h\nu/kT}}{(e^{h\nu/kT} - 1)^2} d\nu \quad (8)$$

where E_{conf} is the configurational energy, $g(T,\nu)$ is the density of the vibrational states, estimated from the power spectrum of the atomic velocity autocorrelation function, and n_f is the number of degrees of freedom for single molecule (being the C−H and C−C bond fixed, n_f = 30). The E_{conf} was obtained from the NPT simulations at 298 and 322 K and 1 bar (the numerical derivative was calculated in this interval) by the quantity[46]

$$E_{conf} = E_{pot} - E_{kin} \quad (9)$$

The calculated C_P value is C_P = 125.0 J mol^{-1} K^{-1}, with a contribution of 37.5 J mol^{-1} K^{-1} for the configurational part and 87.5 J mol^{-1} K^{-1} coming from the vibrational part. The comparison with the experimental value[49] of 157.09 J mol^{-1} K^{-1} is reasonable. Introducing the quantum correction for the C−C and C−H bonds, estimated from the partition function for an harmonic quantum mechanical oscillator using calculated normal modes frequencies,[50] the value increase of ≈ 15 J mol^{-1} K^{-1}.

Isothermal Compressibility. The isothermal compressibility β_T was estimated from the finite difference relationship:

$$\beta_T = -\frac{1}{V}\left(\frac{\delta V}{\delta P}\right)_T = \frac{1}{\rho}\left(\frac{\delta \rho}{\delta P}\right)_T = \left(\frac{\delta(\ln\rho)}{\delta P}\right)_T \approx \left(\frac{\ln\left(\frac{\rho_2}{\rho_1}\right)}{P_2 - P_1}\right)_T \quad (10)$$

where ρ_1 and ρ_2 and P_1 and P_2, are, respectively, the densities and the pressures obtained from two simulations at the same temperature but different pressures. The value calculated at 298 K between 1 and 100 bar was 9.19 × 10^{-5} bar^{-1} which is in good agreement with the experimental value[1] of 9.28 × 10^{-5} bar^{-1}. The values calculated using the upper equation between the two pressure ranges of 1−50 and 50−100 bar were 9.66 × 10^{-5} and 8.68 × 10^{-5} bar^{-1}, respectively. These values are still comparable with the experimental value.[1] An estimation of β_T was also calculated from the fluctuations of the box volume using the relation[51]

$$\beta_T = \frac{\langle \delta V^2 \rangle}{\langle V \rangle kT} \quad (11)$$

where δV is the fluctuation term of the volume V. At 298 K, the resulting value is 10.6 × 10^{-5} bar^{-1}, again in good agreement with the previously reported experimental value.

However, when considering calculated quantities from the box fluctuations, most probably longer simulations can be required to gain a better convergence of the values.[52]

Thermal Expansion Coefficient. The thermal expansion coefficient was evaluated using the following numerical derivative:

$$\alpha_P = \frac{1}{V}\left(\frac{\delta V}{\delta T}\right)_P \approx -\left(\frac{\ln\left(\frac{\rho_2}{\rho_1}\right)}{T_2 - T_1}\right)_P \tag{12}$$

and also estimated from the fluctuations in the volume of the system using the relation[51]

$$\alpha_P = \frac{\langle \Delta H \Delta V \rangle}{\langle V \rangle kT^2} \tag{13}$$

where H is the "instantaneous enthalpy" of vaporization and V is the volume. For the calculation of this value, simulations at 298, 322, and 350 K, were used. The value calculated using eq 12 between the two temperature ranges of 298−322 and 322−350 K were 1.27×10^{-3} and 1.40×10^{-3} K^{-1}, respectively. These values are in good agreement with the experimental value[1] of 1.05×10^{-3} K^{-1}. The value of α_P calculated from the fluctuation formula in eq 13 was nearly 0.95×10^{-3} K^{-1} in the whole temperature range considered. Most likely this different value with the numerical derivation can be in part due to the temperature and pressure coupling schemes used, which may have suppressed the fluctuations in the system and/or longer simulations, which might be required to obtain convergence when using the fluctuation formula (see last comments in the Isothermal Compressibility paragraph).

Hydration Free Energy. The hydration free energy, ΔG_{hyd}, was estimated using the thermodynamic integration method.[53] In this approach, the Hamiltonian (H) of the system is made a function of a coupling parameter λ, for which when $\lambda = 0$, the system corresponds to state A, and when $\lambda = 1$, the system corresponds to state B. In this way the change in free energy can be calculated by

$$\Delta G_{BA} = \int_0^1 G'(\lambda)\, d\lambda = \int_0^1 \left\langle \frac{\partial H}{\partial \lambda} \right\rangle d\lambda \tag{14}$$

where the angular brackets $\langle\ \rangle$ denote averaging over an equilibrium ensemble generated with $H(\lambda)$. The integral in eq 14 was evaluated by obtaining ensemble averages over 30 discrete λ points and determining the integral numerically. At each λ point, 50 ps of equilibration and 300 ps of sampling were performed. Numerical instabilities that can occur during the disappearance of atoms, were avoided by using a soft-core interaction function[54,55] as described by Daura et al.[56] The ΔG_{hyd} was calculated by inserting and deleting a toluene molecule in a box of 800 SPC water molecules. The calculation was performed by switching off the nonbonding interactions between the toluene molecule and the water molecules. The simulations were performed at constant pressure (1 bar) at 298 K. A value of -5.80 ± 0.72 kJ mol^{-1} was calculated for the depletion direction while a value of -5.95 ± 0.70 kJ mol^{-1} was calculated for the insertion one. Both values are in reasonable agreement with the experimental value[57,58] of -3.22 kJ mol^{-1}. The difference between the depletion/insertion directions is 0.15 kJ mol^{-1}, a value which is well inside the error. This make us more confident of the obtained values, based on the considerations of Kofke.[59−63] To get an accurate evaluation of the free energies, the general guidelines referring to the insertion direction should be preferred to the depletion one together with a multistage calculation. Because of the small dimensions of the molecule, we have been able to perform the evaluation in both directions with an high number of λ steps with long equilibration times, which is the basic reason for the small difference between the two obtained values. For comparison, calculated ΔG_{hyd} values using different force fields are reported.[64] In AMBER(ff94),[65] the calculated[64] value is $\Delta G_{hyd} = 0.42 \pm 0.17$ kJ mol^{-1}, CHARMM22[66] results[64] in $\Delta G_{hyd} = 0.38 \pm 0.17$ kJ mol^{-1}, and in OPLS-AA[19] the value is[64] $\Delta G_{hyd} = -2.26 \pm 0.17$ kJ mol^{-1}. All previous models have been optimized under the TIP3P water model, while we have used the SPC[38] water model. The experimental value of $\Delta G_{hyd} = -3.22$ kJ mol^{-1}has been taken from Bennaim et al.[57] and Plyasunov et al.[58] These data (experimental) show a variation[64] between the different authors of 0.54 kJ mol^{-1}, in the same range of error of our calculated value. Compared to the other force fields, the ΔG_{hyd} of the new toluene model here proposed shows a better agreement toward the experimental data. The random statistical error in the $\langle \partial H/\partial \lambda \rangle$ has been estimated using the block averaging method,[51] whereas the total error on the free energy has been obtained by applying the propagation error formula.[67]

3.2. Dynamic Properties. Tracer Diffusion Coefficients. The tracer diffusion coefficients (D) have been calculated using the Einstein relation[51] from the slope of the center of mass mean square displacement (msd) of toluene molecules. The msd was calculated for each toluene molecule in the simulation box using multiple starting points (each every 75 ps) on the last 2.0 ns simulation time to evaluate the msd curve. The use of separated starting points improves the statistics of the curve and reduces the effects of correlations on the computed value of D.[51] The resulting average msd curve was used to estimate the slope by linear regression, omitting the first 5 ps of the msd curve, that contains the collisional part of the diffusion curve. The calculated value of D under reaction field conditions at 298 K was $2.600 \pm 0.084 \times 10^{-5}$ cm^2 s^{-1}, in good agreement with the experimental data of 2.3×10^{-5} cm^2 s^{-1}.[68,69] Using a cutoff treatment instead of a reaction field correction, the D was $2.700 \pm 0.087 \times 10^{-5}$ cm^2 s^{-1}. Considering the error, there is little influence of the electrostatic treatment as underlined in other weakly polar solvents, where the interactions beyond the 1.4 nm are negligible. Simulations performed under the same aforementioned conditions, but with a bigger box of 432 toluene molecules, have given the same results.

Shear Viscosity. The shear viscosity was calculated in the range of the selected temperature and pressure as shown in Table 4. The selected method described by Berendsen[70,71] estimates the viscosity of the liquid from a nonequilibrium simulation in which an external shear-stress acceleration field of the form

$$a_{i,x} = A \cos\left(\frac{2\pi z_i}{l_z}\right) \tag{15}$$

with $a_{i,x}$ being the acceleration in the x direction, A the acceleration amplitude, z_i the z-coordinate of the particle, and l_z the length of the box in the z-direction, is applied to the system. The external acceleration field induces a velocity gradient of the same shape. Under these conditions, for a classical (Newtonian) fluid, the dynamic viscosity (η) is simply given by

$$\eta = \frac{A}{\upsilon}\sigma\left(\frac{l_z}{2\pi}\right)^2 \tag{16}$$

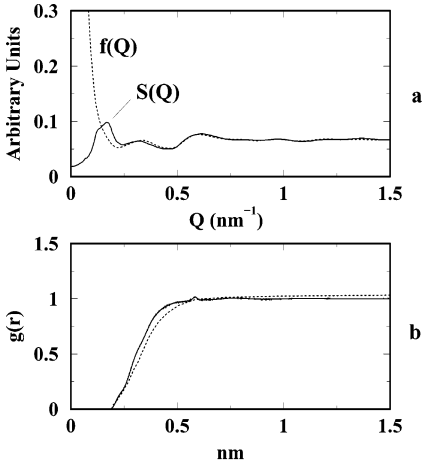

Figure 2. (a) Total structure factor $S(Q)$ (solid line) and intramolecular structure factor, $f(Q)$ (dotted line). (b) Calculated (solid line) and experimental $g(r)$ functions (dotted line).

where σ is the density of the system and v is the resulting velocity amplitude. The A parameter must be carefully selected as the box edge in the z-direction,[70,71] in order to induce a perturbation to the system that can be discernible from thermal velocities but is still small enough to prevent the appearance of order in the fluid. A rectangular box with dimensions of 3.25 $\times$ 3.25 $\times$ 9.75 nm and 575 toluene molecules and a value for A of 0.002 nm ps^{-2} was used. The values of v were calculated as described from Berendsen and Hess.[70,71] The errors have been calculated from the block averaging method.[71] The values of η obtained from the simulations compared to the experimental ones[2] are reported in Table 4. In the pressure and temperature range of 1−100 bar and 298 K, σ is 130.2 μPa s, $\sigma(\%) = 22.3\%$, and the mean deviation is 130.0 μPa s; at 322 K σ is equal to 132.4 μPa s, $\sigma(\%) = 29.7\%$, and the mean deviation is 132.3 μPa s. At a temperature of 350 K (1−100 bar) $\sigma = 83.0$ μPa s, $\sigma(\%) = 24.2$, and the mean deviation is 83.0 μPa s. The reported deviations, considering also other solvent models used in MD,[24,71] show a good behavior of the toluene model.

3.3. Structural Properties. Liquid Structure. The intermolecular radial pair distribution functions,[51] denoted by $g_{xy}(r)$, are calculated from the simulation in the range of the selected temperatures and pressures, for different pairs of atoms. When given, the running integration number (RIN)

$$n_{xy} = 4\pi r_0 \int_0^R g_{xy}(r) r^2 \, dr \qquad (17)$$

where ρ_0 is the number density of the atoms of kind y, is reported. The RIN gives the average number of atoms y contained in a sphere of radius R centered on atom x. The experimental neutron scattering data,[72,73] in liquid toluene at 1 bar and 298 K, are reported in Figure 2a. The total structure factor $S(Q)$ and the intramolecular form factor $f(Q)$, are reported. To compare the obtained all-atom calculated $g(r)$ with the experimental one, the fast Fourier transform of the $S(Q)-f(Q)$ function has been performed[72,73] (Figure 2b). A good agreement between the calculated and the experimental data was found. In Figure 3, the site−site radial distribution functions between the aromatic atoms are reported. For the aromatic carbons (upper panel), the resulting $g(r)$ is similar to what has been found by simulations and X-ray diffraction data of benzene.[12] In the case of the $g(r)$ between the aromatic carbons and hydrogens (middle panel) or aromatic hydrogens (lower panel), no significant structure is present, in line with the benzene results.[12] Figure 4 reports the $g(r)$ between the aliphatic carbons of the methyl

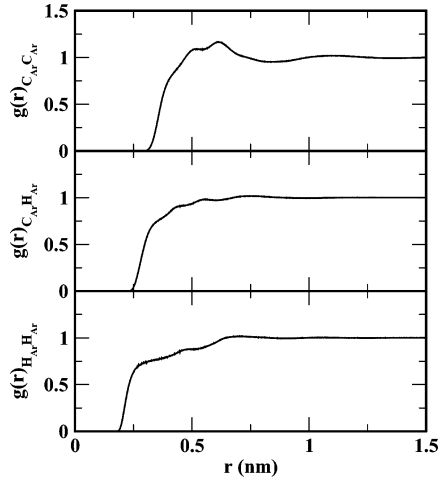

Figure 3. Upper panel: Radial distribution functions, $g(r)$, between aromatic carbons, $C_{Ar}C_{Ar}$. Middle panel: Aromatic carbons and hydrogens, $C_{Ar}H_{Ar}$. Lower panel: Aromatic hydrogens, $H_{Ar}H_{Ar}$.

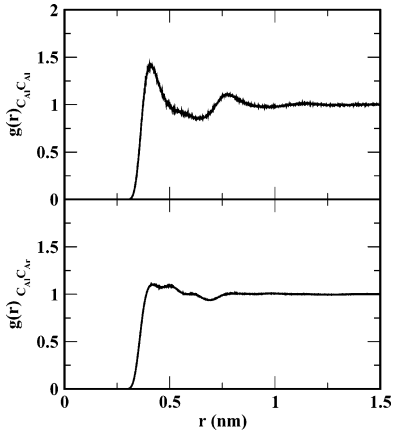

Figure 4. Upper panel: Radial distribution functions, $g(r)$, between methyl carbons, $C_{Al}C_{Al}$. Lower panel: Methyl and aromatic carbons, $C_{Al}C_{Ar}$.

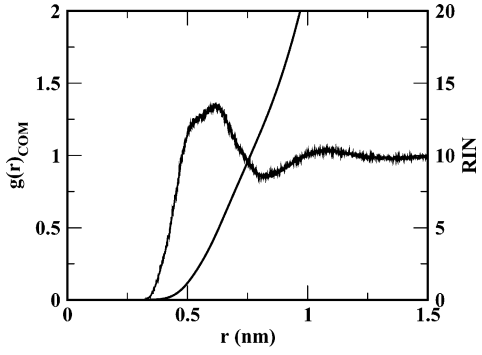

Figure 5. Radial distribution function, $g(r)$ and running integration number (RIN), between mass centers, COM, of toluene molecules.

groups (upper panel) and between the aromatic and aliphatic carbons (lower panel). While in the latter there is no evidence of structure, in the former case a well evident first peak exists at 0.41 nm and a second one at 0.77 nm. An analysis done through the mass center of the toluene molecule (COM), which is nearly coincident with the benzene carbon attached to the methyl group, Figure 5, shows a first broad peak at 0.61 nm and a second less defined peak at 1 nm. The RIN integrated to the first minimum at 0.81 nm yields 12 molecules. This COM $g(r)$ behavior suggests a "cage structure" around each single molecule, as found in some detailed studies on the benzene

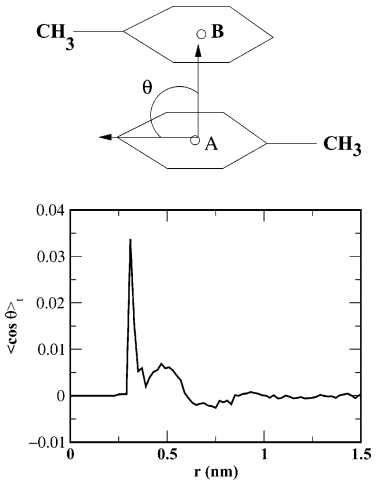

Figure 6. Upper panel: Geometrical definition of the angle θ for the calculation of the reciprocal orientations between toluene molecules. Lower panel: Reciprocal orientations of toluene molecules in the liquid.

liquid structure.[13] These information can be well corroborated analyzing the reciprocal orientations of toluene molecules as shown in Figure 6. The $\langle \cos \theta \rangle_t$ function averaged on the simulation time t, is defined through the θ angle (Figure 6, upper panel) formed between the vector lying on the plane defined by the aromatic carbons and having its origin in the center of the ring (A) and the vector joining this origin with the corresponding center of another toluene molecule (B), defined as aforementioned. The first peak at 0.31 nm has a value of 0.03 (average angle 88°). At this distance the integration number is 1. At longer distances the average angle falls rapidly to 0°, denoting a lack of structure after the first neighbor, being the angle averaged on a higher number of molecules. From the definition of the θ angle, the aforementioned value at 0.31 nm indicates a prevalence of the parallel stacking between dimers of toluene molecules in the liquid phase. This result is in agreement with gas-phase calculations performed on toluene dimers, where the stacked slipped antiparallel configuration (with the ring centers not superimposed and the methyl groups pointing to opposite directions) is the predominant form.[8] This behavior differs from benzene, where the T-shaped form is the stable one (together with the slipped stacked configuration) in the gas-phase and in the liquid[12,74] due to the quadrupolar−quadrupolar interactions.[8,10] Out of the first neighbor, the liquid structure of toluene seems to have no clear structure, as in the case of benzene.[8,13]

Dimer Structure in the Gas Phase. The relative stability of the toluene dimer conformers was considered. Starting conformations were kept from the liquid simulations. For the minimization procedure, holonomic constraints based on the relative distance between the benzene ring centroids and the vector orientation passing through the benzene centroid and the methyl carbon were selected. A total of 10000 conformations were extracted and sampled from the liquid simulation. As the T-shaped complex was not found in the liquid simulation, it was selectively designed, as found in Gervasio et al.[8] and Chipot et al.[10] Previous results of Gervasio et al.[8] and Chipot et al.[10] reported an higher stability of the stacked dimers compared to the T-shaped form. Besides, by the analysis of Gervasio et al.,[8] the T-shaped geometry was discarded as a possible higher minimum in energy compared to the stacked one,[8] with the stacked antiparallel dimer (i.e., the CH_3 groups pointing to the opposite directions) more stable compared to the parallel one of 3.35−3.76 kJ mol^{-1}. In the model here proposed, the most stable conformer was found in the antiparallel stacked geometry, 1.82 kJ mol^{-1} lower in energy compared to the parallel one (see Figure 7). The T-shaped dimer, also in our case, was not found as a minimum. Performing a conjugate gradient minimization starting from the T-shaped complex, the final result was always an antiparallel or parallel stacked conformer (Figure 7). This result is in line with the findings of Gervasio et al.[8] Although the model was mainly parametrized to reproduce the liquid thermodynamic and kinetic properties of toluene, the agreement with previous ab initio and molecular mechanics (AMBER) calculations[8] is reasonable.

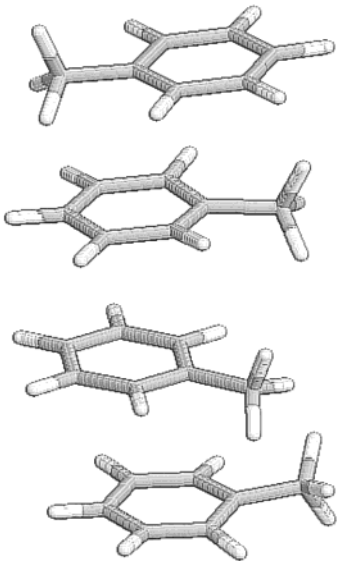

Figure 7. Upper panel: Toluene dimer in antiparallel stacking conformation. Lower panel: Toluene dimer in parallel stacked conformation.

4. Conclusions

A molecular dynamics study of liquid toluene has been presented. The aim is to reproduce the thermodynamic and kinetic properties of the liquid in a wide range of pressure and temperature ($298 < T$ (K) < 350 and $0.1 < P$ (MPa) < 10), important for industrial processes or in organic synthesis. The densities, enthalpies of vaporization, and viscosities have been selected as reference variables for the parametrization of the toluene model. All the other thermodynamic or kinetic quantities have been used as control for the validation of the model. To reach the target under the GROMOS96 force field, new atom types for the aromatic and aliphatic hydrogens and carbons have been introduced. During the parametrization procedure, a difference between aromatic and aliphatic atoms in the LJ parameters has allowed us to reproduce a better agreement with the experimental thermodynamic and kinetic properties in the large range of pressures and temperatures considered. As general tendency, the model underestimates the intermolecular interactions, showing a lower enthalpy of vaporization and lower viscosity compared to the experimental values. The free energy of hydration (ΔG_{hyd}) at 1 bar and 298 K was found to be −5.8 kJ mol^{-1}, in good agreement with the experimental value of −3.6 kJ mol^{-1}. The structural analysis has revealed stacked antiparallel dispositions of the toluene molecules only for the first neighbor and a not well-defined ordered structure already in the first shell. In the temperature and pressure ranges considered, the structural properties of toluene seem not to be affected. Further developments and studies are in progress with

extended simulations on polymer, dendrimeric, and organometallic systems.

Acknowledgment. Gratitude is expressed to Avantium Technologies (Amsterdam) for financial support and to Prof. Christiane Alba-Simionesco (CNRS URA, France) for the neutron scattering data on liquid toluene.

References and Notes

(1) Rubio, J. E. F.; Baonza, V. G.; Taravillo, M.; Nunez, J.; Caceres, M. *J. Chem. Phys.* **2001**, *115*, 4681−4688.
(2) Krall, A. H.; Sengers, V. *J. Chem. Eng. Data* **1992**, *37*, 349−355.
(3) Harris, K. R. *J. Chem. Eng. Data* **2000**, *45*, 893−897.
(4) Döss, A.; Hinze, G. *J. Chem. Phys.* **1997**, *107*, 1740−1743.
(5) Chang, Y. J.; Castner, E. W. *J. Phys. Chem.* **1996**, *100*, 3330−3343.
(6) Sturz, L.; Dölle, A. *J. Phys. Chem. A* **2001**, *105*, 5055−5060.
(7) Ronne, C.; Jensby, K.; Loughnane, B. J.; Fourkas, J.; Faurskov Nielsen, O.; Keiding, S. R. *J. Chem. Phys.* **2000**, *113*, 3749−3756.
(8) Gervasio, F. L.; Chelli, R.; Procacci, P.; Schettino, V. *J. Phys. Chem. A* **2002**, *106*, 2945−2948.
(9) Chipot, C.; Maigret, B.; Pearlman, D. A.; Kollman, P. A. *J. Am. Chem. Soc.* **1996**, *118*, 2998−3005.
(10) Chipot, C.; Jaffe, R.; Maigret, B.; Pearlman, D. A.; Kollman, P. A. *J. Am. Chem. Soc.* **1996**, *118*, 11217−11224.
(11) Kim, J. H.; Lee, S. H. *Bull. Korean Chem. Soc.* **2002**, *23*, 441−446.
(12) Jorgensen, W. J.; Severance, D. L. *J. Am. Chem. Soc.* **1990**, *112*, 4768−4774.
(13) Chelli, R.; Cardini, G.; Procacci, P.; Righini, R.; Califano, S. *J. Chem. Phys.* **2000**, *113*, 6851−6863.
(14) Moe, N. E.; Ediger, M. D. *Macromolecules* **1995**, *28*, 2329−2338.
(15) Kim, J. H.; Lee, S. H. *Bull. Korean Chem. Soc.* **2002**, *23*, 447−453.
(16) Penna, G. L.; Carbone, P.; Carpentiero, R.; Rapallo, A. *J. Chem. Phys.* **2001**, *114*, 1876−1886.
(17) Wick, C. D.; Martin, M. G.; Siepmann, J. I. *J. Phys. Chem. B* **2000**, *104*, 8008−8016.
(18) Jorgensen, W. L.; Madura, J. D.; Swenson, C. J. *J. Am. Chem. Soc.* **1984**, *106*, 6638−6646.
(19) Jorgensen, W. L.; Maxwell, D. S.; Tirado-Rives, J. *J. Am. Chem. Soc.* **1996**, *118*, 11225−11236.
(20) Siepmann, J. I.; Karaborni, S.; Smit, B. *Nature (London)* **1993**, *365*, 330−332.
(21) Martin, M. G.; Siepmann, J. I. *J. Am. Chem. Soc.* **1997**, *119*, 8921−8924.
(22) Chen, B.; Potoff, J. J.; Siepmann, J. I. *J. Phys. Chem. B* **2001**, *105*, 3093−3104.
(23) Fioroni, M.; Burger, K.; Mark, A. E.; Roccatano, D. *J. Phys. Chem. B* **2000**, *104*, 12347−12354.
(24) Fioroni, M.; Burger, K.; Mark, A. E.; Roccatano, D. *J. Phys. Chem. B* **2001**, *105*, 10967−10975.
(25) Walser, R.; Mark, A. E.; van Gusteren, W. F.; Lauterbach, M.; Wipff, G. *J. Chem. Phys.* **2000**, *112*, 10450−10459.
(26) Dang, L. X. *J. Chem. Phys.* **2000**, *113*, 266−273.
(27) Borodin, O.; Smith, G. D. *J. Phys. Chem. B* **2003**, *107*, 6801−6812.
(28) van der Spoel, D.; Berendsen, H. J. C.; van Buuren, A. R.; Apol, E.; Meulenhoff, P. J.; Sijbers, A. L. T. M.; van Drunen, R. *Gromacs User Manual*; Department of Biophysical Chemistry, University of Groningen: Groningen, The Netherlands, 1995.
(29) van Gunsteren, W. F.; Billeter, S. R.; Eising, A. A.; Hünenberger, P. H.; Krüger, P.; Mark, A. E.; Scott, W. R. P.; Tironi, I. G. *Biomolecular Simulation: The GROMOS96 Manual and User Guide*; vdf Hochschulverlang, ETH Zürich: Zürich, Switzerland, 1996.
(30) Lee, C.; Yang, W.; Parr, R. G. *Phys. Rev. B* **1988**, *37*, 785−789.
(31) Becke, A. D. *J. Chem. Phys.* **1993**, *95*, 5648−5642.
(32) Hehre, W. J.; Ditchfield, R.; Pople, J. A. *J. Chem. Phys.* **1972**, *56*, 2257−2261.
(33) Frisch, M. J.; et al. *Gaussian 98, Revision A.3*; Gaussian, Inc.: Pittsburgh, PA, 1998.
(34) Breneman, C. M.; Wiberg, K. B. *J. Comput. Chem.* **1990**, *11*, 361−397.
(35) Carlson, H. A.; Nguyen, T. B.; Orozco, M.; Jorgensen, W. *J. Comput. Chem.* **1993**, *14*, 1240−1249.
(36) Weiner, S.; Kollman, P. A.; Case, D. A. *J. Comput. Chem.* **1986**, *7*, 230.
(37) Miller, K. J.; Savchik, J. A. *J. Am. Chem. Soc.* **1979**, *101*, 7206−7213.
(38) Berendsen, H. J. C.; Postma, J. P. M.; van Gusteren, W. F.; Hermans, J. Interaction Models for Water in Relation to Protein Hydration. In *Intermolecular Forces*; Pullmann, B., Ed.; Reidel: Dordrecht, The Netherlands, 1981.
(39) Gusteren, W. F. V.; Daura, X.; Mark, A. E. *Helv. Chim. Acta* **2002**, *85*, 3113−3130.
(40) Hoover, W. G. *Phys. Rev. A* **1985**, *31*, 1695−1697.
(41) Parrinello, M.; Rahmann, A. *Phys. Rev. Lett.* **1980**, *45*, 1196−1199.
(42) Riddick, J. A.; Bunger, W. B.; Sakano, T. K. *Organic Solvents: Physical Properties and Methods of Purification*; John Wiley and Sons: New York, 1986; Vol. 2.
(43) Hess, B.; Bekker, H.; Berendsen, H. J. C.; Fraaije, J. G. E. M. *J. Comput. Chem.* **1997**, *18*, 1463−1472.
(44) Miyamoto, S.; Kollman, P. A. *J. Comput. Chem.* **1992**, *13*, 952−962.
(45) Majer, V.; Svoboda, V. *Enthalpies of Vaporization of Organic Compounds: A Critical Review and Data Compilation;* Blackwell Scientific Publications: Oxford, England, 1985.
(46) Chelli, R.; Procacci, P.; Cardini, G.; della Valle, R. G.; Califano, S. *Phys. Chem. Chem. Phys.* **1999**, *1*, 871−877.
(47) Stillinger, F. H.; Weber, T. A. *Phys. Rev. A* **1982**, *25*, 978−989.
(48) Stillinger, F. H. *J. Phys. Chem.* **1984**, *88*, 6494−6499.
(49) Grolier, J.; Roux-Desgranges, G.; Berkane, M.; Jimenez, E.; Wilhelm, E. *J. Chem. Thermodyn.* **1993**, *25*, 41−50.
(50) Herzberg, G. *Molecular Spectra and Molecular Structure. II. Infrared and Raman Spectra of Polyatomic Molecules*; Van Nostran Reinhold Company: New York, 1945.
(51) Allen, M. P.; Tildesley, D. J. *Computer Simulations of Liquids;* Oxford Science Publications: Oxford, England, 1987.
(52) Jorgensen, W. L. *Chem. Phys. Lett.* **1982**, *92*, 405−410.
(53) van Gunsteren, W. F.; Daura, X.; Mark, A. E. Free Energy Perturbation Calculations. In *Encyclopaedia of Computational Chemistry 2*; Schleyer, P. v. R., Ed.; John Wiley & Sons: Chichester, England, and New York, 1998.
(54) Beutler, T. C.; Mark, A. E.; van Schaik, R. C.; Gerber, P. R.; van Gunsteren, W. F. *Chem. Phys. Lett.* **1994**, *222*, 529−539.
(55) Zacharias, M.; Straatsma, T. P.; McCammon, J. A. *J. Chem. Phys.* **1994**, *100*, 9025−9031.
(56) Daura, X.; Hünenberger, P. H.; Mark, A. E.; Querol, E.; Aviles, F. X.; van Gunsteren, W. F. *J. Am. Chem. Soc.* **1996**, *118*, 6285−6294.
(57) Ben-naim, A.; Marcus, Y. *J. Chem. Phys.* **1984**, *81*, 2016−2027.
(58) Plyasunov, A. V.; Shock, E. L. *Geochim. Cosmochim. Acta* **2000**, *64*, 439−468.
(59) Lu, N.; Singh, J. K.; Kofke, D. A. *J. Chem. Phys.* **2003**, *118*, 2977−2984.
(60) Lu, N.; Kofke, D. A. *J. Chem. Phys.* **2001**, *115*, 6866−6875.
(61) Lu, N.; Kofke, D. A. *J. Chem. Phys.* **1999**, *111*, 4414−4423.
(62) Lu, N.; Kofke, D. A. *J. Chem. Phys.* **2001**, *114*, 7303−7311.
(63) Lu, N.; Adhikari, J.; Kofke, D. A. *Phys. Rev. E* **2003**, *68*, 026122−1.
(64) Shirts, M. R.; Pitera, J. W.; Swope, W. C.; Pande, V. S. *J. Chem. Phys.* **2003**, *119*, 5740−5761.
(65) Cornell, W. D.; Cieplak, P.; Bayly, C. I.; Gould, I. R.; Merz, K. M.; Ferguson, D. M.; Spellmeyer, D. C.; Fox, T.; Caldwell, J. W.; Kollman, P. A. *J. Am. Chem. Soc.* **1995**, *117*, 5179−5197.
(66) MacKerell, A. D.; Bashford, D.; Bellot, M. *J. Phys. Chem. B* **1998**, *102*, 3586−3616.
(67) Bevington, P. R. *Data Reduction and Error Analysis for the Physical Sciences*; McGraw-Hill: New York, 1969.
(68) Pickup, S.; Blum, F. D. *Macromolecules* **1989**, *22*, 3961−3968.
(69) Moe, N. E.; Ediger, M. D. *Macromolecules* **1995**, *28*, 2329−2338.
(70) Berendsen, H. J. C. Transport properties computed by linear response through weak coupling to a bath. In *Computer Simulations in Material Science*; Meyer, M., Pontikis, V., Eds.; Kluwer: Dordrecht, The Netherlands, 1991.
(71) Hess, B. *J. Chem. Phys.* **2002**, *116*, 209−217.
(72) Morineau, D.; Alba-Simionesco, C. *J. Chem. Phys.* **1998**, *109*, 8494−8503.
(73) Teboul, V.; Alba-Simionesco, C. *J. Phys.: Condens. Matter* **2002**, *14*, 5699−5709.
(74) Tsuzuki, S.; Honda, K.; Uchimaru, T.; Mikami, M.; Tanabe, K. *J. Am. Chem. Soc.* **2001**, *124*, 104−112.